Polymer 51 (2010) 3685–3692

Contents lists available at ScienceDirect

Polymer

journal homepage: www.elsevier.com/locate/polymer

Comparison of adipate and succinate polyesters in thermoplastic polyurethanes

Mark F. Sonnenschein*, Steven J. Guillaudeu, Brian G. Landes, Benjamin L. Wendt

The Dow Chemical Co., Corporate Research and Development, Midland, MI 48674, USA

ARTICLE INFO

Article history:
Received 19 February 2010
Received in revised form
21 May 2010
Accepted 7 June 2010
Available online 12 June 2010

Keywords:
Renewable feedstocks
Polyurethane elastomers
Polyesters

ABSTRACT

Succinic acid derived from sugar is reportedly going to be an abundant and inexpensive feedstock for polymer synthesis in the near future. This article reports on succinic acid based polyester polyols prepared with butane diol and compares them to polybutylene adipate, a common polyester polyol derived from petrochemicals. Polybutylene succinate diol prepared via standard condensation polymerization techniques was directly comparable to polybutylene adipate diol. Thermoplastic polyurethanes prepared from succinate and adipate based polyols are compared using differential scanning calorimetry, dynamic mechanical spectroscopy, tensile measurements, wide and small angle X-ray scattering, transmission electron microscopy, atomic force microscopy, and abrasion tests. Thermoplastic polyurethanes made using polybutylene succinate exhibited higher glass transition temperatures and more hard-phase to soft-phase interaction than those with polybutylene adipate, presumably due to the higher number of hydrogen bond accepting carbonyls on the succinate soft segment chain. Abrasion resistance of the elastomers was a strong function of the overall hard segment volume and secondarily a function of factors related to the soft segment, with the succinate based thermoplastic polyurethanes showing a slight decrement relative to the adipate elastomers.

1. Introduction

Exploration of renewable feedstocks for chemicals and materials is increasing due to rising petrochemical costs and the drive to reduce output of greenhouse gases [1]. Succinic acid (SA) which can be obtained from the fermentation of sugars, has been noted as one of the most important value added chemicals from biomass from which many other industrially important chemicals can be derived [2,3]. The total costs associated with obtaining SA from fermentation relative to petrochemical derivation (hydrogenation of maleic acid) is not yet known with precision, but it appears that bio-derived succinic acid can be economically disruptive to aliphatic polyester chemistry if the expected efficiencies are met [4,5].

Little research has been conducted comparing polysuccinates directly to polyadipates and few commercial polymers are based on succinic acid when much cheaper, available and petrochemically derived adipic acid (AA) can be used. In a study of poly(butylene succinate) (PBS) and poly(butylene succinate-co-butylene adipate) (PBSA) of various diacid ratios, it was found that increasing the amount of AA in the polymer from 0% to 60% reduced the polyester melting point from 114 °C to 32 °C, and then from 60% to 100% increased it again to 60 °C for polybutylene adipate (PBA) [6].

Of the polyesters incorporating succinic acid, the most prevalent is PBS. PBS has physical and processing qualities in some respects similar to polyethylene making it more amenable to commercial adoption [7–9]. In the past, the high price of petrochemically derived SA has limited PBS acceptance into general use. However, with potential availability of low-cost SA in the near future, we have explored its application in several functions where AA is conventionally employed. Approximately 2 billion pounds per year of adipate polyester find application in polyurethane systems including elastomers, foams and coatings [10,11]. In this article we compare the function of polybutylene succinate to polybutylene adipate in thermoplastic polyurethanes (TPUs). We detail the synthesis of PBS soft segments and urethane elastomers, and characterize the elastomer morphology by atomic force microscopy (AFM), wide angle X-ray scattering (WAXS), small angle X-ray scattering (SAXS), and transmission electron microscopy (TEM). The elastomer physical properties are measured by differential scanning calorimetry (DSC), dynamic mechanical spectroscopy (DMS), tensile measurements, and DIN abrasion.

2. Experimental

Unless otherwise noted, all materials were obtained from Aldrich (Milwaukee, WI) and used as-received. Polybutylene adipate of Mn 1000 and 2000 g/mol molecular weight was obtained

* Corresponding author. Tel.: +1 989 636 7415; fax: +1 989 626 4019.
E-mail address: mfsonnenschein@dow.com (M.F. Sonnenschein).

0032-3861/$ – see front matter © 2010 Elsevier Ltd. All rights reserved.
doi:10.1016/j.polymer.2010.06.012

from Chemtura Corporation (Middlebury, CT) as Fomrez 44-111 and 44-57 respectively. 4,4′-Methylene diphenyl diisocyanate (MDI) was stored in a freezer to limit dimerization, and allowed to warm to room temperature before opening. 1,4 Butane diol (BDO) was dried in a vacuum oven or over 4 Å molecular sieves prior to use. Dibutyl tin dilaurate was obtained from Air Products (Allentown, PA).

3. Synthesis of PBS

The desired products are diols with very high levels of terminal hydroxyl. This is accomplished by applying the Carothers equation determining the ratio of monomers to obtain the desired product. This simplifies to:

$$\text{Moles BDO/moles SA} = 1 + 1/n$$

n is determined by considering one unit of BDO as a chain initiator and the monomer unit to be the condensation unit of (SA + BDO − $2H_2O$). Thus the target Mn is calculated as:

$$\text{Mn} = \text{MW}_{\text{BDO}} + n \cdot \text{MW}_{\text{monomer}} = 90.12 + n \cdot 172.18$$

$$n = \text{moles monomer/moles initiator}$$
$$= \text{moles SA/(moles BDO} - \text{moles SA)}$$

PBS samples were prepared by polycondensation of SA with BDO using dibutyl tin dilaurate or dibutyl tin oxide as catalyst. No difference was observed between materials using either catalyst. Samples of either Mn = 1000 g/mol or 2000 g/mol were synthesized for comparison to commercial polybutylene adipate samples.

SA and BDO were added to a 3-necked flask fitted with an N_2 inlet, a thermocouple connected to a home-made temperature controller and a Dean–Stark trap. The flask and trap were wrapped with insulation for reaction efficiency and the N_2 flow was maintained at a level to remove the condensation product and minimize loss of BDO from the mixture. The components minus the catalyst were heated to 110 °C and then 0.1% catalyst was added to the stirring liquid using a Teflon coated magnet. The mixture was gradually heated to 180 °C in 10 °C increments to maintain a steady rate of condensate production. The reaction was monitored by determining the acid number (ASTM D4662-08). The reaction was stopped when the acid number was below 2 mg KOH/g polymer, preferably below 1 mg KOH/g polymer which normally took less than 2 days. GPC and ^{1}H NMR were subsequently run on the bulk polymer at this point (Fig. 1). NMR of the samples usually allowed calculation of Mn quite close to the expected values and in agreement with OH number. GPC of the samples using an Agilent GPC with a Polymer Labs Mixed E (2 in series) column with a chloroform eluent and a polystyrene determined calibration curve suggested Mn values at variance with the NMR for both PBS and PBA. Subsequent polymerization of thermoplastic polyurethanes was based on the NMR determined hydroxyl number.

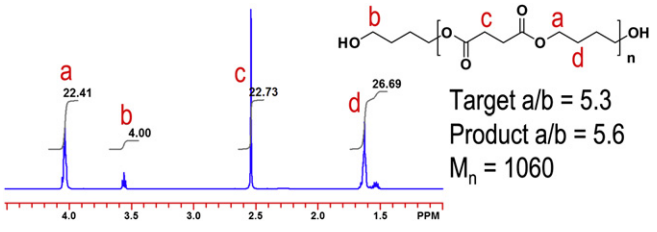

Fig. 1. Representative ^{1}H NMR of PBS in $CDCl_3$.

4. Synthesis of TPU

TPUs were prepared in a Haake dispersive mixer at 30%, 40%, and 47% (wt%) hard segment by finishing the PBS or PBA soft segments with BDO and MDI. Stoichiometry was strictly followed and a molar excess of 2.5% isocyanate was always used. Soft segment diols were melted at 130 °C and mixed with BDO. MDI was melted in a separate beaker. Once the starting materials had been melted, they were poured all at once into the Haake dispersive mixer which had been preheated to 150 °C. A few drops of dibutyl tin dilaurate catalyst were added, and the temperature set point of the Haake was raised to 200 °C. Once the temperature of the polymer had reached 195–200 °C, the polymer was removed, cut into pieces, and dried overnight in a vacuum oven at 60–70 °C.

Portions of the TPUs (~10 mg) were dissolved in DMF at reflux (~2 mL) and injected (5 μL) on an Agilent HP GPC system with THF as the eluent. The molecular weights were determined by comparison to a standard curve based on linear polyethylene oxide.

Pieces of the PBA TPUs were compression molded at 185 °C first at 2000 lbs pressure for 3 min followed at 100,000 lbs for 3 min, and then allowed to cool under 100,000 lbs for 14 min. PBS TPUs were molded at 155 °C at the same pressures for 1 min, 2 min, and 14 min, respectively. Bars were molded for dynamic mechanical spectroscopy on an ARES II. Materials were initially analyzed in frequency sweep at −60 °C to ensure the strain was in the linear portion of the stress–strain response. Mechanical spectroscopy was then measured using a temperature range from −60 to 175 °C, usually with a frequency of 1 rad/s and 0.3–0.4% strain. Plates were molded and samples were stamped for tensile testing on an Instron using ASTM D412 at 2"/min. Pucks were molded for DIN abrasion testing according to DIN 53516.

PBS TPUs with 30% hard segment, before and after tensile testing, were analyzed by TEM. Each sample was cryogenically polished using a cryo-ultramicrotome. The polished faces were then exposed to RuO_4 vapors for 2 h to stain the samples. After staining, thin sections, approximately 90 nm, were cut and imaged on a JEOL 1230 TEM. The images were captured on a CCD camera.

TPUs with 47% hard segment were analyzed by tapping mode (TM) AFM. Thin sections of samples were prepared with cryomicrotomy and placed on cleaved mica. TMAFM images were obtained on a Digital Instruments MultiMode using a Nanoscope IV controller (software v 6.13). Silicon cantilevers and tips were used (Budget Sensor Multi75, force modulation probes, k ~ 3 N/m, f res ~ 75 kHz). Typical tapping conditions were Ao ~ 2.0 V, Asp ~ 1.0 to 1.5 V, and rsp ~ 0.5 to 0.75, with the tip-surface interaction repulsive in nature.

Samples with 30% hard segment were analyzed by WAXS. Samples with 30% and 40% hard segment and the soft segments were analyzed by SAXS at room temperature with a normal beam transmission mode. A Bruker D-8 Advance θ–θ X-ray diffractometer, equipped with a cobalt sealed-tube source, primary beam monochromator, and Vantec-1 linear position sensitive detector was used for collecting the WAXS patterns. Data were collected from 3 to 90° 2-θ using Co Kα1 radiation (wavelength = 1.788965 Å), a scan rate of 2°/min, an effective step size of 0.017°, and a detector window of 8°. The samples were rotated during data acquisition.

Small angle X-ray scattering (SAXS) analyses for d-spacing were performed using the following procedure. Specimens were cut to a width of 5 mm and a thickness of 3 mm. Conditioning of the X-ray beam was achieved using a multi-layer optic and triple pinhole collimation. All samples were analyzed under vacuum in normal beam transmission mode. Cu k_{avg} radiation λ = 1.54184 Å was employed. An area detector was used to collect the scattering intensities. SAXS exposure time was set for 30 min. Two-dimensional SAXS data sets. The 1-d SAXS data were analyzed using the commercial software platform JADE.

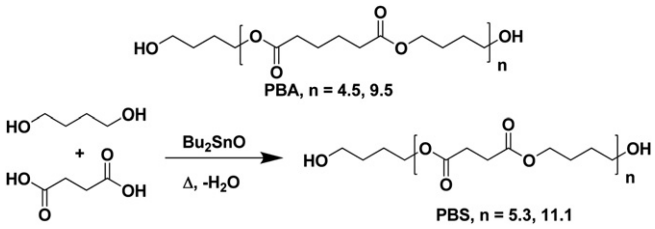

Scheme 1. Preparation of polybutylene adipate and succinate.

DIN abrasion was obtained on a Qualitest (Ft Lauderdale FL) abrasion tester built specifically for performing standard test DIN 53516. Each specimen was preceded and followed by measurement of abrasion on standardized rubber samples to assure accuracy and precision. Abrasion values are ±10% based on precision and ±5% accuracy based on the standard sample calibration.

5. Results and discussion

5.1. Polybutylene succinate and adipate soft segments

Polybutylene adipate (PBA) is a commonly used, low-cost soft segment in TPUs providing clarity, little yellowing, and good abrasion and chemical resistance [12]. PBA of various molecular weights are sold commercially, so we did not synthesize samples of PBA for this study. PBS, however, is only available in high molecular weights as oligomers of PBS chain extended with hexamethylene-diisocyanate so samples with Mn = 1000 and 2000 g/mol were synthesized. (Scheme 1)

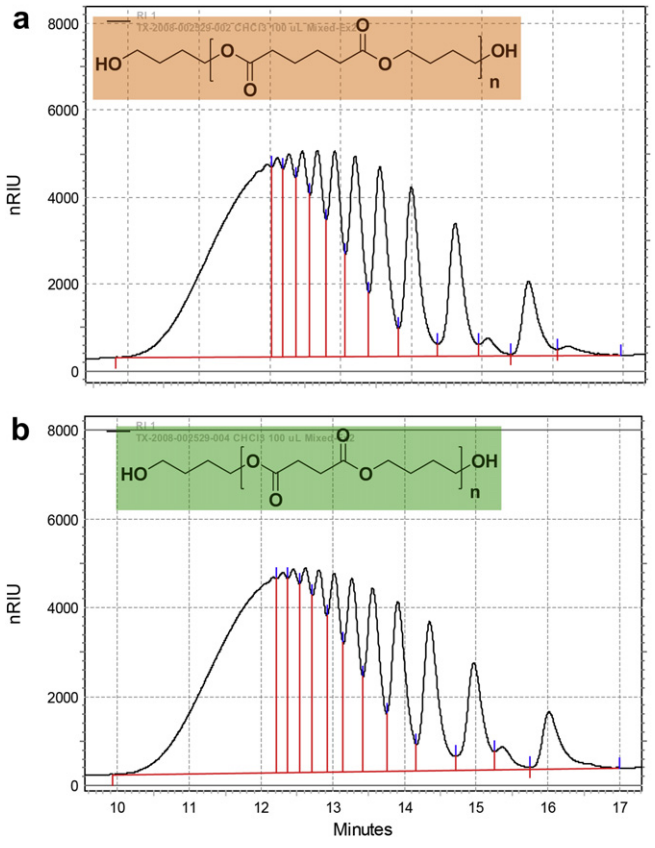

Fig. 2. GPC chromatograms of a) PBA and b) PBS, both ca. Mn 2000 g/mol.

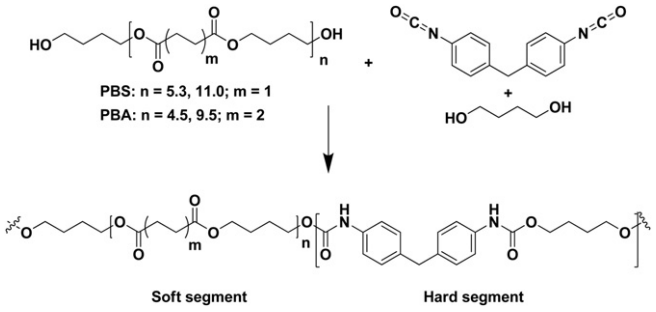

Scheme 2. Synthesis of TPUs.

The tin-catalyzed polycondensation of BDO with SA proceeded without complication. Many polyester syntheses are performed in a two-step process, in which oligomerization occurs at elevated temperatures by removal of water with a nitrogen stream and then higher molecular weight is built by removing excess diol under vacuum at high temperatures. Since we wanted relatively low molecular weight oligomers, molecular weight was controlled by stoichiometry. Therefore, we predicted the final molecular weight of our material by assuming one equivalent of BDO was an initiator, and each monomer unit was comprised of one SA with one BDO, minus two molecules of water. In our synthetic conditions, BDO was not removed under the nitrogen stream, so the ratio of BDO:SA in the final product was the same as added to the flask. Using

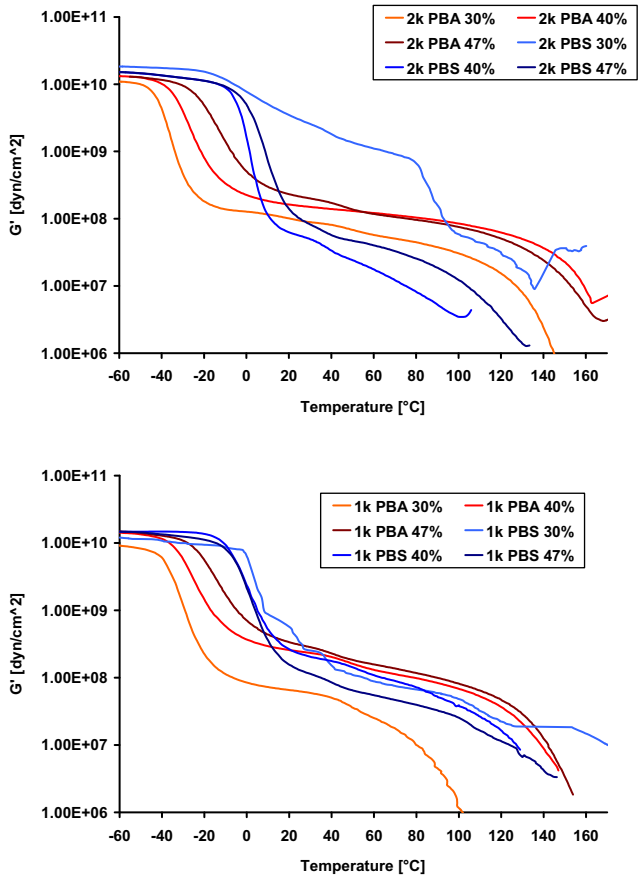

Fig. 3. Dynamic mechanical spectroscopy of adipate and succinate based TPUs as a function of soft segment molecular weight and hard segment content. All shades of blue are PBS, all shades of red are PBA. (For interpretation of the references to colour in this figure legend, the reader is referred to the web version of this article.)

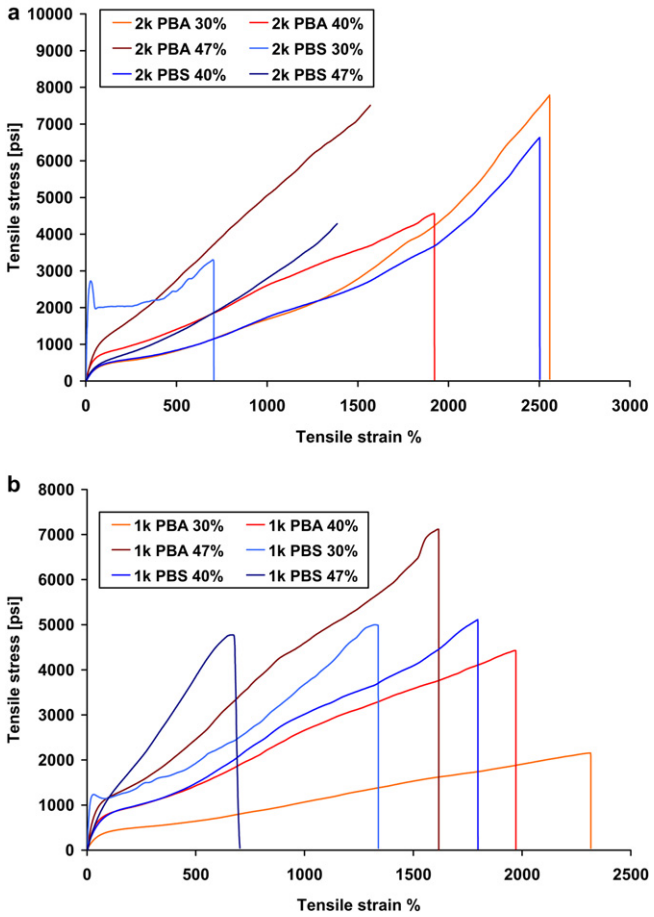

Fig. 4. Stress–strain curves for TPU elastomers as a function of hard segment volume for a) Mn = 2000 Da and b) Mn = 1000 Da soft segments. All shades of blue are PBS, all shades of red are PBA. (For interpretation of the references to colour in this figure legend, the reader is referred to the web version of this article.)

dibutyl tin dilaurate instead of dibutyl tin oxide or succinic acid dimethyl ester instead of SA gave comparable results.

The molecular weight (Mn) of the PBS samples could be determined by analysis of the ^{1}H NMR spectra (see Fig. 1 Experimental section for a representative Spectrum). A comparison of the integrations of the CH_2 at δ 3.6 ppm adjacent to hydroxyl to those of the CH_2 at δ 4.1 ppm adjacent to the ester linkage provided the means to calculate the degree of polymerization. 1000 and 2000 g/mol PBS samples were determined to have Tm's of 100 and 109 °C, respectively, by DSC [8]. To ensure that our PBS had molecular weight distributions similar to the commercial PBA, GPC in chloroform was performed for each sample. As can be seen (Fig. 2), the PBS and PBA samples have almost identical molecular weight distributions. Both polymers are composed of low molecular weight monomers, dimers, and oligomers that cannot be resolved on the GPC system before ~14 min retention time. The molecular weights compared to polystyrene standards are quite similar for the respective PBS and PBA 1000 or 2000 g/mol samples. Experiments in this report utilized polybutylene succinate diols with hydroxyl number determined equivalent weights of 988, 880, 532 and 439 for soft segments in making TPU elastomers. The 988 and 532 equivalent weight materials were used in all cases except where specifically noted.

5.2. Thermoplastic polyurethanes

TPUs were synthesized by premixing soft segment diols with BDO and pouring into a Haake mixer at the same time as premelted 4,4′-methylenebis diphenylisocyanate (MDI). This method is believed by the authors to more closely resemble an extrusion process and result in materials with better elastomeric properties. The resulting TPUs are block copolymers of polyester soft segment and polyurethane hard segment [13–16]. Phase separation in such systems is driven by hydrogen bonding between urethane NH groups and urethane carbonyls on adjacent polymer chains in the hard segment [17]. Because polyesters also contain carbonyls capable of acting as H-bond acceptors, some interaction between phases is expected. Taking this rationale further, because PBS chains have more carbonyls than PBA for a given molecular weight, we expected more interaction between segments of PBS TPUs than those of PBA. TPUs with Mn > 15,000 and most often >20,000 Da were typically obtained. (Scheme 2)

During compression molding, we found that PBS TPUs were not as stable at typical molding temperatures (185 °C) as PBA TPUs. Many bubbles were present in PBS TPUs after molding. GPC analysis of the PBS TPUs after molding at 185 °C indicated a distinct loss of

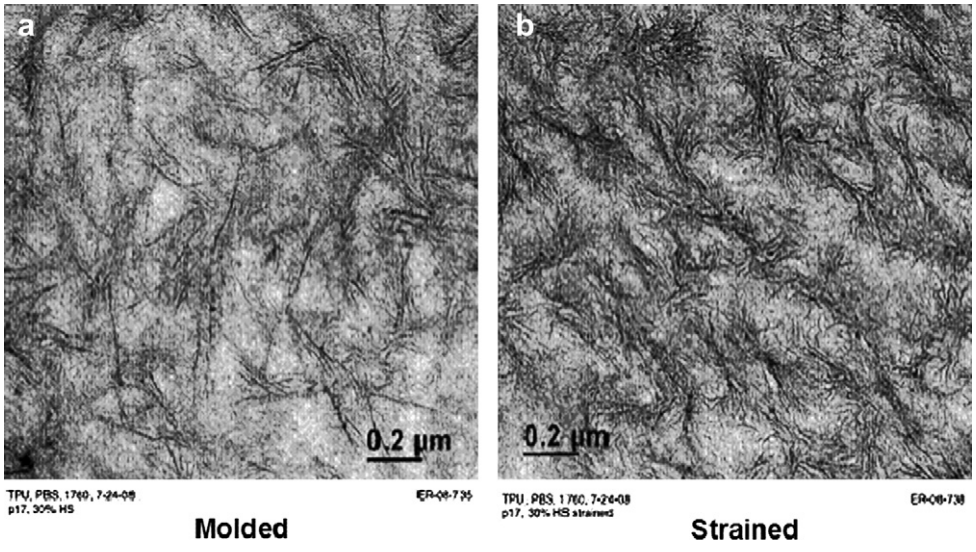

Fig. 5. TEM micrographs of 30% hard segment elastomers made with Mn = 2000 Da polybutylene succinate soft segments a) after compression molding and b) after straining to break. Strain direction is diagonal across the picture.

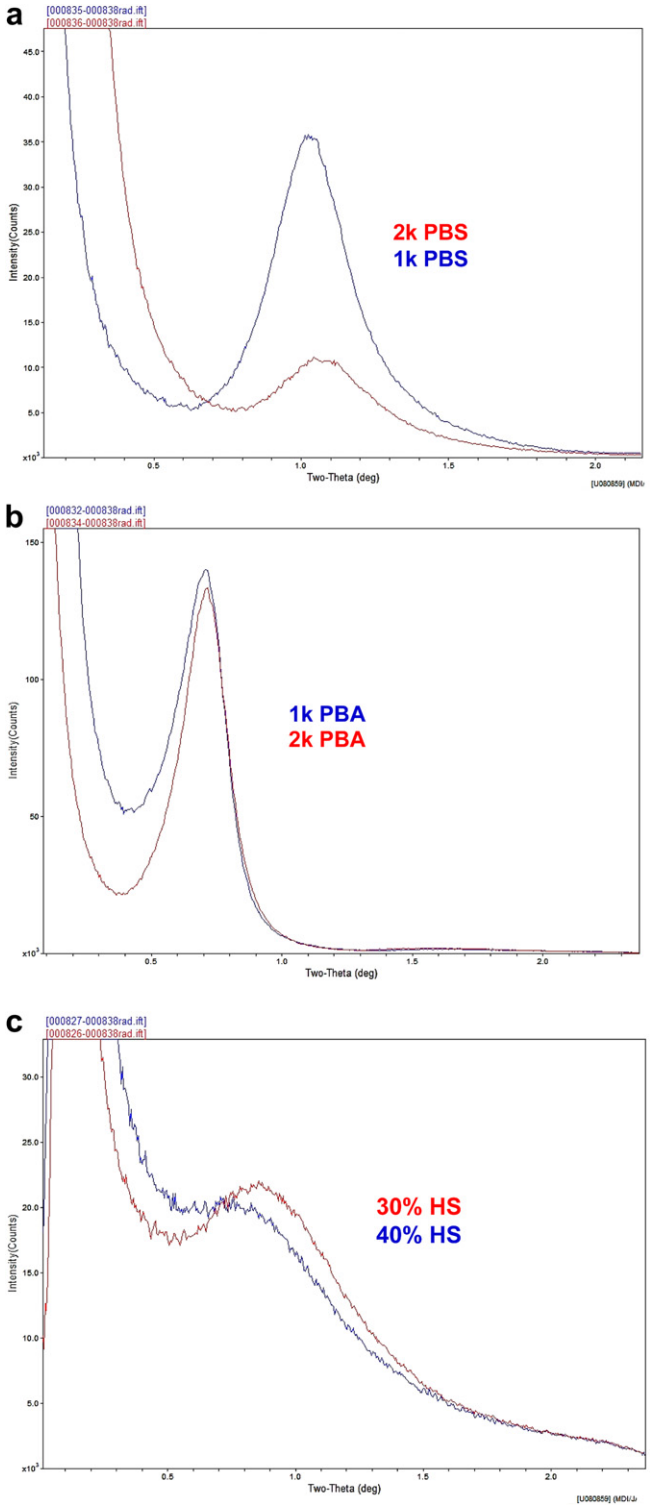

Fig. 6. SAXS scattering spectra of a) PBS, b) PBA, and c) PBS TPUs.

molecular weight (25–75% loss). After trying a range of temperatures, it was determined 155 °C was best for molding the PBS TPUs. Thermogravimetric analysis of materials showed the PBS TPU degradation onset was consistently 2–17 °C lower than that of the analogous PBA TPUs, but all were found to degrade above 295 °C, well above the temperatures used during compression molding. DSC analysis of two 40% hard segment TPUs did not indicate

Table 1
Hard segment d-spacing distances in Å. D is calculated from the formula $d = \lambda/(2\sin\theta)$ where θ is obtained from data such as obtained in Fig. 5. PBS samples with low hard segment volumes have an additional contribution from soft segment crystallinity.

SAMPLE	%Hard Segment	PEAK	CENTROID
1 kg PBS		86	83
2 kg PBS		82	80
TPU/1 kg PBS	30	112	102
TPU/1 kg PBS	40	94	85
TPU/2 kg PBS	30	102	94
TPU/2 kg PBS	40	107	100
TPU/1 kg PBA	30	122	112
TPU/1 kg PBA	40	122	114
TPU/2 kg PBA	30	124	
TPU/2 kg PBA	40	117	
1 kg PBA		125	129
2 kg PBA		123	126

a difference at higher temperatures that may have given insight into a reaction occurring. We do not know the cause of PBS TPU thermal instability. We believe it could be due either to a higher number of acid end groups in the lab-synthesized PBS attacking polymer ester bonds to form anhydrides, which would be unstable to residual water at elevated temperatures, or it could be that commercial PBAs are supplied with thermal stabilizers.

Dynamic mechanical spectroscopy of TPUs provides evidence of increased phase mixing in PBS containing materials (Fig. 3). Typical TPU elastomer behavior is observed for the PBA samples. Their Tg's and moduli at room temperature increase as the percentage hard segment is increased. PBS TPUs do not show trends different from PBA except the 30% hard segment PBS TPU was not elastomeric due to extensive crystallinity of the soft segment [18,19]. This soft segment crystallinity led to a higher RT modulus than those of the 40% or 47% hard segment PBS materials. PBS TPUs with 40% and 47% hard segment did behave like typical elastomers, showing the trend of PBAs: higher Tg and higher modulus with more hard segment. PBS TPUs had higher Tg's than PBA TPUs, presumably because increased H-bonding between PBS and hard segment results in decreased mobility of the PBS chains as well the intrinsically higher Tg of PBS relative to PBA (−33 °C vs. −60 °C respectively) [6]. (Tan delta spectra for the samples are provided in supplemental on-line information). Tm's of the TPUs show the opposite trend – higher Tm's for PBA TPUs – for the same reason. The increased PBS interaction with hard segment is essentially an impurity in the hard segment, which lowers the hard segment melting point.

Fig. 4 is complementary data to Fig. 3. The very high strain to break of these materials indicates they all have high molecular weight [20]. The stress–strain data confirm that elastomer modulus is a function of hard segment volume, soft segment molecular weight, and soft segment crystallinity. This crystallinity aspect is especially true for PBS based elastomers at low hard segment volumes. These materials, especially at 30% hard segment and Mn 2000 Da soft segment, exhibit thermoplastic behavior with a yield strain and necking. Similar behavior is also observed for the 1000 Da PBS soft segments but the relatively lower molecular weight of the soft segment and the increased phase mixing resulting from shorter hard segment lengths inhibits the growth of soft segment crystals. The morphology responsible for elastomer strain hardening at low and high strain with a semi-crystalline soft segment is evidenced in Fig. 5. The lamellar structure of PBS in the 30% hard segment thermoplastic matrix are random and unorganized prior to straining to break as seen in Fig. 5a. After straining, the crystals appear to align in the direction of strain and perhaps organize into sheath structures (Fig. 5b). It is possible that the initial excess modulus response of the 30% hard segment thermoplastics results from resistance of the crystals to re-orientation and that the

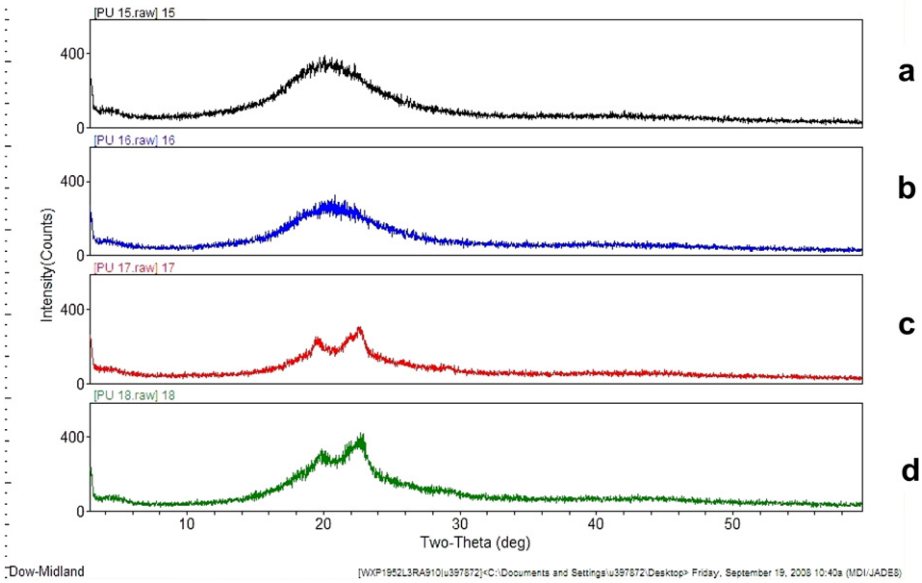

Fig. 7. WAXS spectra of 30% (wt) hard segment TPUs from PBA a) Mn = 1000 Da b) Mn = 2000 Da and PBS c) Mn = 1000 Da d) 2000 Da.

final high strain hardening occurs as the lamellae organize into additional virtual crosslink points. At higher hard segment volumes, soft segment crystals, which nucleate and grow after hard segment formation, are unable to cross the hard segment barriers and don't form either due to steric inhibition, or due to vitrification of the elastomer network as the hard segment network forms.

Two of the elastomers, PBA with 30% hard segment and PBS with 40% hard segment (Fig. 4), possess remarkably similar shapes including apparent strain hardening. This suggests that equivalent hard segment structure can be obtained for PBS and PBA elastomers, but hard segment volume must be increased with PBS to obtain equivalence due to increased interaction of PBS and hard segment.

To further elucidate the effect of carbonyl spacing on PBS and PBA based TPU elastomers, small angle X-ray analysis was undertaken [21–26]. Fig. 6 shows representative scattering spectra for PBS and PBA as well as spectra for two TPU samples from PBS. Table 1 provides numerical values for the structural variables of interest.

The PBA and PBS soft segments exhibit well defined scattering defining hard segment spacing. PBS, with greater overall volume crystallinity than PBA, has a smaller inter-crystallite spacing reflecting the smaller volume percentage amorphous content [27]. Scattering from PBA and PBS derived TPUs arises from phase separated hard segment. Scattering from PBS TPUs is a convolution of both the hard-phase segregation and crystallinity within the soft segment. Fig. 7 is a WAXS comparison of 30% hard segment TPUs from PBA and PBS showing the crystalline contribution of PBS at low hard segment, while the PBA maintains an amorphous morphology. Elastomers with 40% (wt) hard segment and above are amorphous independent of soft segment.

TPU SAXS from PBS and PBA follow trends consistent with their respective soft segment effects on morphology. Elastomers comprised of PBS have smaller d-spacing (smaller inter-domain distance). This is most likely due to the smaller and more poorly formed hard segments in PBS compared to those in PBA at similar hard segment content, and due to the convolution of inter-lamellar distances within the soft segment phase. One could anticipate a greater contribution to the SAXS from the hard segment contrast because of its greater volume fraction and greater density difference compared to its surroundings. This is observed indirectly in the SAXS data and directly via microscopy (vide infra).

Analysis of the tail of the SAXS scattering, the Porod region [22–26], can provide insight into the interfacial boundary between soft and hard segments. For a perfectly sharp interfacial boundary, the scattering intensity should decay as a function of q^{-4}. Deviations of this exponent indicate interfacial phase mixing. The absolute values of the exponent in this relationship for PBS and PBA based TPUs are shown in Fig. 8. It is observed that PBS TPUs have Porod constant of 2.6–3.2, while those of PBA are closer to the theoretical sharp boundary value of 4, ranging from 3.5 to 3.9. This indicates that the interface between the PBS soft segment and the MDI/BDO hard segment is more diffuse than the interface in PBA TPUs. Again, contributions to this measure will arise from the order within the soft segment phase, however; due to its lower volume fraction and smaller contrast we would expect this contribution to be minor. Microscopy shows this morphology even more dramatically.

Fig. 9 is AFM images of TPU elastomers from PBA and PBS with 47% weight polyurethane hard segment. At this hard segment volume no soft segment crystallinity is observed by either DSC or X-ray analysis so observed structure is a reflection of hard segment morphology. What is clearly observable in Fig. 9 is the relative coarseness of the co-continuous hard segment

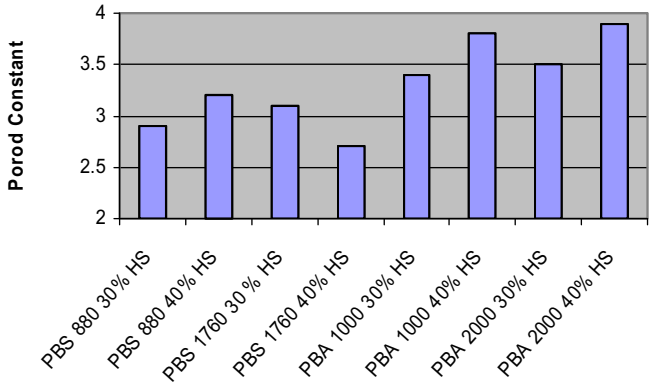

Fig. 8. Comparison of Porod constants for elastomers made from PBA and PBS. (All values are ±0.2).

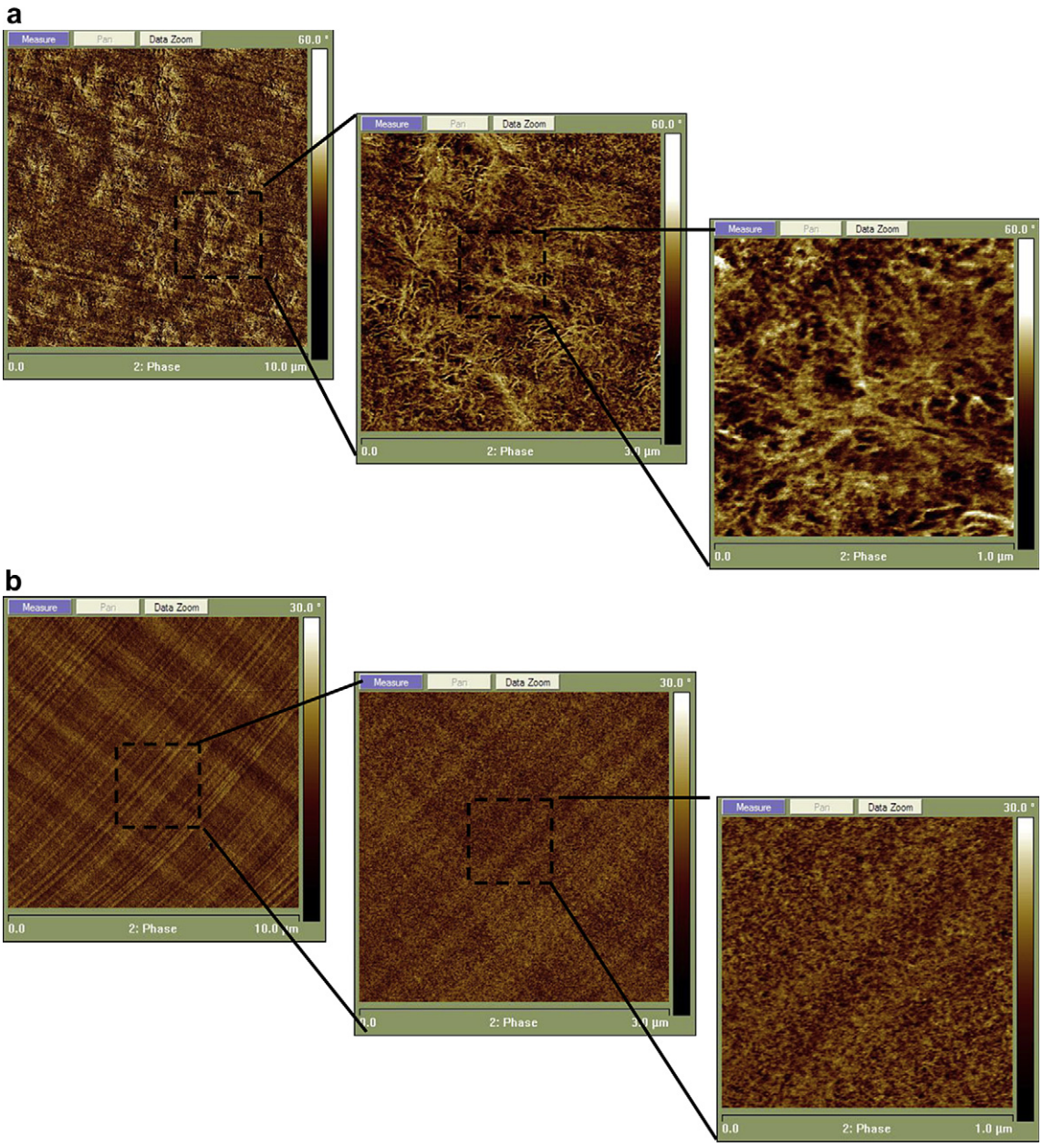

Fig. 9. AFM phase contrast images of a) PBA and b) PBS TPU elastomers with 47% (wt) hard segment. Scale is shown at the bottom axis of each image with image width ranging from 10 to 3 to 1 μm for each series.

structure in the PBA elastomer. The PBS elastomer shows a highly dispersed hard segment structure that is significantly phase mixed with the soft segment (dark in the images). This is consistent with 1) SAXs analyses showing smaller hard segment d-spacing, 2) Porod analysis showing more diffuse interface between the hard and soft phases, and 3) the higher glass transition temperatures of the PBS elastomers. A coarser hard segment structure for the PBS soft segment TPUs are obtainable, but we and others [28,29], have observed this to result when the mixing during synthesis is insufficient to achieve an equilibrium distribution. In these cases a somewhat lower soft segment Tg can also be observed.

Another way of comparing TPUs with different structures is testing performance in practical use-like applications. A common expectation of TPUs is that they be abrasion resistant, commensurate with their use in wheels, footwear, coatings and numerous other high wear applications. The DIN abrasion test [30] is essentially an automated, controlled, and calibrated rubbing of the elastomer by sand paper. From the materials point of view, abrasion is a reflection of the entirety of the material properties including low strain dynamic, high strain tensile, compression, and thermal response [31,32]. Fig. 10 compares DIN abrasion data for the elastomers as a function of hard segment volume and the soft segment. Data obtained on PBA elastomers is consistent with known values for these elastomers. Elastomers made with PBS and PBA are comparable in their abrasion performance with a slight advantage of PBS elastomers when made from low molecular weight soft segments, and a more significant advantage for PBA elastomers when made of high molecular weight soft segments. This practical result is likely a reflection of the better hard segment

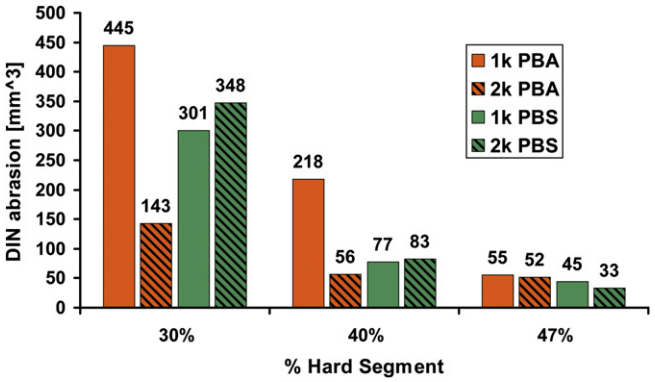

Fig. 10. DIN abrasion of TPU from polybutylene adipate and succinate as a function of soft segment molecular weight and hard segment volume.

phase separation of PBA elastomers which is going to be most pronounced at high soft segment molecular weights.

6. Conclusion

A comparison of material properties of thermoplastic polyurethane elastomers made with petrochemically derived polybutylene adipate and potentially sugar derived polybutylene succinate was presented. PBA was in all cases amorphous in elastomers having 30% or greater hard segment by weight. The higher percent crystallinity of PBS is manifest in soft segment properties when the hard segment volume is less than 40%. The lamellar crystals have a significant effect on properties resulting in thermoplastic rather than elastomeric properties. The greater density of H-bond accepting carbonyl groups on the PBS chain result in increased hard segment–soft segment interactions than PBA based elastomers. The increased interactions are evident in higher PBS glass transition temperatures, lower hard segment melting points, and smaller inter-lamellar hard segment spacing. The magnitude of the difference translates to slightly inferior abrasion properties in elastomers with lower hard segment volumes or lower soft segment molecular weights.

Acknowledgements

We would like to thank Dr. Greg Meyers for the AFM images and Dr. Robert Cieslinski for the TEM images.

Appendix. Supplementary data

Supporting information associated with this article can be found, in the online version, at doi:10.1016/j.polymer.2010.06.012.

References

[1] Anastas PT, Warner JC. Green chemistry: theory and practice. New York: Oxford University Press; 1998.
[2] Werpy T, Frye J, Holladay. Succinic acid – a model building block for chemical synthesis from renewable resources. In: Kamm JB, Gruber PR, Kam M, editors. Biorefineries – industrial processess and products: status quo and future directions, vol. 1. Weinheim: Wiley–VCH; 2006. 367379.
[3] Song H, Lee SY. Enzym Microb Tech 2006;39:352–61.
[4] Dornburg V, Herman BG, Patel MK. Environ Sci Technol 2008;42:2261–7.
[5] Caesar B. Ind Biotechnol 2008;4:50–4.
[6] Ahn BD, Kim SH, Kim YH, Yang JS. J Appl Polym Sci 2001;82:2808–26.
[7] Huang X, Li C, Zheng L, Zhang D, Guan G, Xiao Y. Polym Inter 2009;58:893–9.
[8] Papageorggiou GZ, Bikaris D. Polymer 2005;46:12081–92.
[9] Liu Y, Ranucci E, Soderquist-Lindblad M, Albertsson A-C. J Polym Sci Part A Polym Chem 2001;39:2508–19.
[10] Linak E, Kishi A. Alkyd/Polyester surface coatings CEH Marketing research report #592.6000 Pub: chemical Economics Handbook – SRI; 2007.
[11] Polyurethanes VI. Whippany, NJ: Skeist Incorporated; July 2006.
[12] Singh A, Weissbein L, Mollica JC. Rubber Age 1966;98:77–83.
[13] Blackwell J, Gardner K. Polymer 1979;20:13–7.
[14] Chu B, Gao T, Li Y, Wang J, Desper CR, Byrne CA. Macromolecules 1992;25:5724–9.
[15] Garrett JT, Siedlecki CA, Runt J. Macromolecules 2001;34:7066–70.
[16] Camberlin Y, Pascault JP. J Polym Sci Polym Phys Ed 1984;22:1835–44.
[17] Elwell MJ, Mortimer S, Ryan AJ. Macromolecules 1994;27:5428–39.
[18] Sonnenschein MF, Lysenko Z, Brune DA, Wendt BL, Schrock AK. Polymer 2005;46:10158–66.
[19] Korley LT, Pate BD, Thomas EL, Hammond PT. Polymer 2006;47:3073–82.
[20] Bueche F. Physical properties of polymers. New York: Interscience Publishers; 1962 [Chapter 2].
[21] Sonnenschein MF, Prange R, Schrock AK. Polymer 2007;48:616–23.
[22] Sonnenschein MF, Wendt BL, Schrock AK, Sonney J-M, Ryan AJ. Polymer 2008;49:934–42.
[23] Kim M-H. J Appl Cryst 2004;37:643–51.
[24] Martin DJ, Meijs GF, Renwick GM, McCarthy SJ, Gunatillake PA. J Appl Polym Sci 1996;62:1377–86.
[25] Ophir Z, Wilkes GL. J Polym Sci Polym Phys Ed 1980;18:1469–80.
[26] Koberstein JT, Morra B, Stein RS. J Appl Cryst 1980;13:34–5.
[27] Clough SB, Schneider NS, King AO. J Macromol Sci-Phys 1968;B2:641–8.
[28] Ahn TO, Choi IS, Jeong HM, Cho K. Polym Internat 1993;31:329–33.
[29] Sanchez-Adsuar MS, Papon E, Villenave J-J. J Appl Polym Sci 2000;76:1590–5.
[30] DIN 53515 testing of rubber, elastomers; Determination of abrasion resistance 6/87.
[31] Schocke D, Arastoopour H, Bernstein B. Powder Technol 1999;102:207–14.
[32] Gurvich MR. J Elast Plast 2007;39:53–67.